Temperature dependence of thermal positron branching at metal surfaces

P. A. Huttunen,* J. Mäkinen, D. T. Britton,† E. Soininen,‡ and A. Vehanen§
Laboratory of Physics, Helsinki University of Technology, SF-02150 Espoo 15, Finland
(Received 20 February 1990)

The positron and positronium emission yields are measured as a function of temperature at Cu(111) and Al(110) surfaces having a negative positron work function, and at the positive-work-function surfaces Ag(100) and Ag(111). At the Cu(111) positron (e^+) emission yield is reduced at low temperatures, vanishing as $T \rightarrow 0$ K. The positronium (Ps) emission exhibits a similar temperature dependence at Cu(111) and Al(110). The dominating temperature-dependent feature at these negative-e^+-work-function surfaces is the reflection of the e^+ wave from the surface potential. Using a simple one-dimensional model we obtain estimates for the transition rates for surface trapping, e^+, and Ps emission to be of the order of 10^3 m/s. Ps-emission probabilities for Ag(100) and Ag(111) surfaces show drastically different temperature behavior. In order to explain these results we propose a new surface-trapping mechanism, the acoustic-phonon-mediated trapping. This would imply a weak temperature dependence of Ps emission at Ag surfaces.

I. INTRODUCTION

Positrons (e^+) are increasingly applied to probe surface and near-surface phenomena, following the progress in the production of positron beams (for a recent review see Ref. 1). Many of the electron techniques used extensively in surface science have their counterparts in the positron physics. Low-energy positron diffraction (LEPD) (Ref. 2) has been speculated to have certain advantages over low-energy electron diffraction (LEED), e.g., lack of the exchange interactions should make it easier to calculate the intensity distributions in LEPD than in LEED. Molecular vibrations on the surface can be studied with the reemitted-positron energy-loss spectroscopy (REPELS),[3] and recently it has been demonstrated that positron-induced Auger-electron emission[4] has some benefits compared to conventional Auger spectroscopy. By measuring the momentum distribution of positronium (Ps) atoms emitted from the surface, the surface electron density of states can be examined.[5] Further, positron localization into the lattice defects provides a unique technique of detecting defects in the near-surface region.[6]

In positron-beam experiments positrons are implanted with keV energies inside the solid. After the rapid thermalization, a fraction of the positrons diffuses back to the surface prior to annihilation. For a thermal positron approaching the surface from inside the metal, the most common processes, shown schematically in Fig. 1, are the following:

(i) Emission as a free positron from the surface.[7] For thermal positrons this will occur if the e^+ work function ϕ_+ is negative, which is the case for most metals. At clean metal surfaces the reemitted positrons are almost all elastic, having a narrow energy distribution limited by the thermal energy.[8,9]

(ii) Formation and emission of a positronium (Ps) atom by direct pickup of a near-surface electron.[10] Ps emission is energetically allowed if the binding energy of the Ps atom (6.8 eV) is larger than the sum of the electron and positron work functions. Owing to the electronic screening in metals, Ps is formed at the low-electron-density tail outside the outermost atomic layer, and the capture of an electron has been found to occur nonadiabatically, leading to a continuous kinetic energy spectrum of Ps.[11]

(iii) Trapping into a surface state induced by the image interaction. Positron capture is followed either by annihilation in this state or thermal excitation from the surface as a Ps atom.[12]

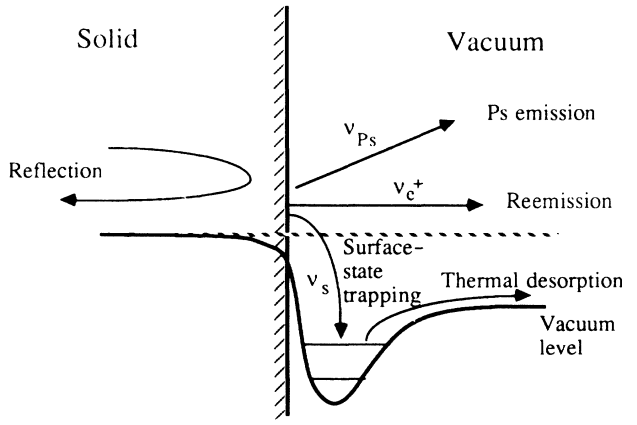

FIG. 1. Schematic picture of thermal positron-surface interaction mechanisms shown for a negative-work-function surface.

(iv) Reflection of the positron wave from the surface potential. The potential step is attractive if the positron work function is negative and repulsive if $\phi_+ > 0$.

Many aspects of the positron-surface interaction are well established. There remain, however, a number of questions of fundamental nature. The character of the surface state is not properly understood. Theoretically, the surface state has been described either as an image-potential induced surface state[13,14] or a physisorbed Ps-like state.[15] The experiments[5] do not support either of these models, but suggest a lateral localization of the positron at the surface possibly due to the surface defects and impurities. The measured Ps momentum distributions show an enhanced component at low momentum,[7,5] the origin of which is still unknown. We are also lacking an overall theory of the positron-surface interaction, though there are many model calculations.

Furthermore, the transition rates at the surface are not known, and the role of the internal reflection of the positron wave approaching the surface from inside the metal has long been a subject of controversy. Quantum-mechanical reflection from the one-dimensional surface potential was proposed by Nieminen and Oliva.[16] As the thermal positron wave vector $\mathbf{k} \rightarrow 0$, the reflectivity should approach unity, in agreement with the well-known wave mechanical result for a step potential. Accordingly, the surface should become fully opaque at 0 K for any abruptly changing surface potential, and the e^+ and Ps yields should vanish at low temperatures. The early experiments[17,18] failed, however, to observe the predicted decrease in the escape probability as the temperature decreases. In a recent experiment[19] positron reflection was found at the Cu(111) surface.

We have studied the thermal positron branching as a function of temperature from the Cu(111), Al(110), Ag(100), and Ag(111) surfaces. The Cu(111) and Al(110) surfaces both have a negative positron work function. At the Cu(111) surface both e^+ and Ps emission yields vanish at low temperatures. The same is observed for Ps emission at the Al(110). The temperature behavior is consistent with the reflection of the positron wave from the surface potential. We have estimated the surface transition rates considering the transmission of a plane wave through the effective single-particle potential of a positron near the surface. This simple approach, which reproduces the observed temperature dependencies, gives the transition rate $\nu_s \sim 10^3$ m/s for the capture into the surface state, and around 300 K the e^+ and Ps emission rates of the same order are obtained. The values are in good accord with theoretical predictions.[20–22] Ps yields at the positive-work-function surfaces Ag(100) and Ag(111) differ from each other below 200 K. Besides the reflection, an enhanced capture rate into the surface state could be a principal reason for the reduced Ps yield in the low-temperature limit, and the difference between Ag(100) and Ag(111) is discussed in terms of different mechanisms of surface-state trapping.

Positron surface processes are analogous to many atomic and electronic phenomena occurring at the surface. The low-energy reflection and sticking of atoms has been a subject of long-term discussions.[23] Ps emission resembles to some extent photoemission.[24,5] The choice between the emission as a free positron or a Ps atom is analogous to the ion neutralization process occurring at the surface (see, e.g., Ref. 25). Positrons offer a possibility to obtain complementary information on these processes and their quantum nature.

The paper is organized as follows. In Sec. II the thermal e^+ and Ps yields and the transition rates are introduced. The experimental details are reported in Sec. III, and the results are presented in Sec. IV. In Sec. V we consider the surface processes at positive- and negative-work-function surfaces in the light of the experimental results, and also extract estimates for the different transition rates. Section VI contains the discussion of the results. The paper is concluded in Sec. VII.

II. POSITRON AND POSITRONIUM YIELDS

A. Diffusion model and surface transition rates

Measurements of the positron branching ratios are almost exclusively based on the determination of the probability of positron diffusion to the surface. A simple yet fairly successful way of describing thermal positron motion in solids starts from the diffusion-annihilation equation (see, e.g., Ref. 1). At the surface ($z=0$) the positron density $n(z,t)$ is subject to the boundary condition

$$D_+ \frac{\partial n(z,t)}{\partial z}\bigg|_{z=0} = \nu n(z=0,t) , \tag{1}$$

where D_+ is the positron diffusion coefficient and ν represents the total escape rate at the surface. This condition simply requires that the positron flux at the surface is equal to the escape rate. The overall probability of the positron, implanted at incident energy E, escaping from the sample prior to annihilation is[16]

$$J(E) = \int dt\, \nu n(z=0,t) = \frac{\nu}{\nu + L_+/\tau} \int_0^\infty dz\, P(z,E) e^{-z/L_+} . \tag{2}$$

In Eq. (2) τ is the positron lifetime in the bulk, $L_+ = (D_+\tau)^{1/2}$ is the one-dimensional diffusion length, and $P(z,E)$ is the positron stopping profile, representing the positron density distribution at $t=0$. The model is limited to positrons implanted at depths of several scattering mean free paths (typically 20 Å at room temperature), and it appears that the assumptions underlying the use of the diffusion equation are valid except at very low incident positron energies or sample temperatures.[26]

Throughout this work the stopping profile of keV positrons is taken as

$$P(z,E) = -\frac{d}{dz} \exp\left[-\left[\frac{z}{z_0} \right]^2 \right] , \tag{3}$$

with $z_0=(\alpha/\rho)[E/(1\text{ keV})]^n$, where ρ is the mass density. The stopping profile is based upon Monte Carlo simulations of positron slowing down[27] and measurements of multilayer structures.[28] Those studies also yield the parameters $n=1.5-1.6$ and $\alpha=4.5-4.6\ \mu\text{g cm}^{-2}$, almost independent of the target material. The values adopted here are $n=1.55$ and $\alpha=4.5\ \mu\text{g cm}^{-2}$.

In Eqs. (1) and (2) the total escape rate ν represents the rate of all surface processes removing the positron from the metal. Usually in low-energy positron experiments the rate ν is considered both constant and large compared to L_+/τ, corresponding to a perfectly absorbing surface. This is justified as the escape rate only appears as a prefactor in Eq. (2), not affecting the positron diffusion properties, as long as the branching ratios remain unaltered. At low temperatures, however, thermal positrons are reflected from the surface potential, making ν finite, and the escape processes become limited by the transition rate.[19] At high temperatures the escape eventually becomes diffusion limited, i.e., almost all positrons returning to the surface escape to vacuum.

The total positron transition rate ν at the surface can be divided in various ways, corresponding to the different surface processes. Positrons that are lost through the surface escape either as a free e^+ (ν_{e^+}) or a Ps atom (ν_{Ps}) or they are trapped into the image-induced surface state (ν_S). The measured energy distributions of the reemitted positrons at clean metal surfaces correspond to the thermal distribution, indicating an elastic escape process.[8,9] In metals, Ps is formed in the low-electron-density region outside the surface by pickup of a surface electron. Positronium time-of-flight (PsTOF) (Refs. 11 and 29) and two-dimensional angular correlation[5] measurements give evidence that the electron capture is a sudden process leaving an electron hole in the metal, and it can be described in terms of a single-particle picture. The reemission and Ps emission rates are thus combined into a surface transmission rate ν_T. Consequently, the total transition rate is

$$\nu=\nu_T+\nu_S=\nu_{e^+}+\nu_{\text{Ps}}+\nu_S\ . \tag{4}$$

Although the different transition rates have not been known, it has been a relatively common observation that at room temperature the division is approximately equal between e^+ emission, Ps emission, and surface trapping.

The positron and positronium yields, subject to a direct measurement, can be expressed as a function of the incident positron energy in terms of $J(E)$ in Eq. (2) and the transition rates ν_{e^+} and ν_{Ps} at the surface as

$$f_{e^+}(E)=\frac{\nu_{e^+}}{\nu}J(E)\ , \tag{5a}$$

$$f_{\text{Ps}}(E)=\frac{\nu_{\text{Ps}}}{\nu}J(E)\ . \tag{5b}$$

We have not included the thermal Ps emission in Eq. (5), since we are considering temperatures below the threshold for thermal desorption from the surface state. A similar expression can be written for the fraction of positrons localized to the surface state, but, unlike for positron and positronium emission, there is no direct way of measuring this transition probability with the experimental setup. The prefactors ν_{e^+}/ν and ν_{Ps}/ν in Eq. (5) represent the surface branching ratios for e^+ and Ps emission. To extract the experimental transition rates, the e^+ and Ps yields are extrapolated to zero incident energy:

$$f_{e^+}(0)=\frac{\nu_{e^+}}{\nu_S+\nu_T+L_+/\tau}\ , \tag{6a}$$

$$f_{\text{Ps}}(0)=\frac{\nu_{\text{Ps}}}{\nu_S+\nu_T+L_+/\tau}\ . \tag{6b}$$

Based upon elementary wave-mechanical considerations, Nieminen and Oliva[16] predicted the direct positron emission to be reduced at low temperatures because of increasing reflection of the positron wave approaching the surface potential from inside the metal. In particular, they argued that the e^+ and Ps yields vanish in the limit $T\rightarrow 0$ as the transmission coefficient goes to zero for any surface barrier. This would leave trapping into the surface state the only available channel for the escaping positron. In our Letter[19] we succeeded in observing the internal reflection of thermal positrons at low temperatures at the Cu(111) surface, contradicting the earlier experimental work. The measurement of the temperature dependence also gives estimates for the different transition rates.

B. Measurement of thermal e^+ and Ps yields

For a negative-work-function surface, the e^+ and Ps fractions are measured simultaneously by applying a positive or negative voltage to a grid in front of the sample. Thereby the reemitted positrons are either forced to annihilate in the sample or are allowed to escape the sample surface and the detector region. The reemission yield is given by the difference in the total count rate T between these conditions:

$$f_{e^+}=\frac{T_+-T_-}{T_+}\ . \tag{7}$$

The subscripts denote the grid bias, which is positive (+) or negative (−) with respect to the sample. Alternatively, the reemission yield can be determined from the corresponding Ps fractions f_{Ps}^+ and f_{Ps}^- and the electron pickup probability for returned positrons.[30] The integral energy distribution of reemitted positrons is measured by sweeping the grid bias across the sample potential. Also, the positron work function can be deduced from these measurements.[31,32]

Positronium yields are measured in a standard way by separating 3γ annihilations arising from the decay of ortho-Ps from the 2γ decay of either positrons or para-Ps. Considering the various processes of positron annihi-

lation, it can be shown that the Ps fraction f is given by[33]

$$f=\left[1+\frac{P_1}{P_0}\frac{R_1-R}{R-R_0}\right]^{-1} . \quad (8)$$

The ratio R is defined as $R=(T-P)/P$, where T and P refer, respectively, to the integral counts in the total and peak regions of the γ spectrum. The ratio varies from R_0, when no positronium is formed, to a maximum R_1 when all incident positrons end up as Ps. P_0 and P_1 are the peak counts under those conditions.

The true Ps yield f_{Ps} is given by the fractions f_{e^+} and f_{Ps}^- as

$$f_{\mathrm{Ps}}=f_{\mathrm{Ps}}^-(1-f_{e^+}) . \quad (9)$$

The factor $1-f_{e^+}$ is the probability for a positron to annihilate in the sample region.

Examples of the e^+ and Ps yields, measured from the Cu(111) surface at 370 K, are presented in Fig. 2. The solid lines correspond to the least-squares fits to Eq. (2). Equations (2) and (5) are not valid at low incident energies. A considerable fraction of the measured signal up to a few keV incident energies originates from positrons, which escape before reaching the thermal equilibrium.[34,35] This leads to different transition rates. To extract the *thermal* positron diffusion lengths and their contribution to the surface processes, the low-energy data up to a few keV is omitted.[34] When the contribution from epithermal positrons is correctly accounted for, Soininen *et al.*[36] have shown that the positron diffusion coefficient has the temperature dependence of $T^{-1/2}$, expected from e^+-acoustic phonon scattering theory[37] in the wide temperature range from 20 K to the threshold of thermal vacancy formation. In Fig. 2 the positron diffusion lengths corresponding to the reemission yield f_{e^+} and Ps yields f_{Ps} and f_{Ps}^+ are $L_+=1210\pm120$, 1250 ± 130, and 1250 ± 60 Å, respectively. These are in good accord with the value from the Doppler broadening measurements $L_+=1310$ Å.[36] However, especially at low temperatures, the e^+ and Ps yields become small, making the uncertainty in the L_+ excessively large. Therefore, we have adopted the thermal positron diffusion lengths based upon accurate, high statistics line-shape measurements from the very same crystals.

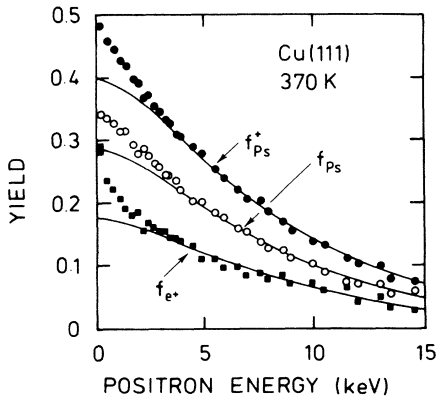

FIG. 2. The reemission yield $f_{e^+}(E)$ and the Ps yields $f_{\mathrm{Ps}}^+(E)$ and $f_{\mathrm{Ps}}(E)$ measured from the Cu(111) at 370 K. Solid lines are least-squares fits to the diffusion model.

III. EXPERIMENT

The variable-energy positron beam used in the experiments is described in detail elsewhere.[38] The β_+ decay positrons emitted from a ^{58}Co source deposited on the tungsten single crystal needle are moderated in a W(110) crystal in the backscattering geometry. W(110) is a negative positron work-function surface and hence a source of positrons of energy $|\phi_+|\sim3.0$ eV with a narrow energy distribution and a small angular spread. The beam is transported to the sample chamber in an axial magnetic field, and accelerated in a linear accelerator to the incident energy 0–30 keV. The intensity of the beam having a diameter of 3 mm and an energy width of less than 3 eV is typically 10^6 e^+/s, corresponding to the overall conversion efficiency 1.5×10^{-3}. The annihilation radiation is monitored with an intrinsic high-purity Ge detector. The sample chamber is equipped with a residual-gas analyzer, a sputter-ion gun, and a combined LEED–retarding field Auger (RFA) system for surface preparation and characterization. The base pressure of the UHV system is 5×10^{-11} mbar.

The metal surfaces investigated are Al(110), Cu(111), Ag(100), and Ag(111). The Al(110) crystal of 99.9999% purity was supplied by Cominco Inc. Cu(111) (99.9999% purity) was cut with a diamond saw from a single crystal rod received from Tampere University of Technology. All silver crystals of purity better than 99.9999% [two pieces of Ag(111) and one Ag(100)] were from Metal Crystal & Oxides, Ltd. Samples were mechanically polished and electrolytically (Al,Cu) or chemically (Ag) etched. Ag crystals were also externally annealed. Samples were cleaned *in situ* by repeated Ar^+-ion sputtering and annealing cycles, and the surfaces were monitored with low-energy electron diffraction (LEED) and Auger-electron spectroscopy (AES). The main contaminant at the Cu(111) crystal was carbon, having a concentration of less than 1 at. %. Oxygen or *sulphur,* which are common contaminants on Cu surfaces,[39] were below the detection limit. On silver surfaces, the most common residual impurities, sulphur, oxygen, and chlorine, were not detected, indicating a concentration of much less than 1 at. %. Evaluation of the carbon concentration on the surface is difficult owing to the overlap of the carbon and silver Auger transition lines around ~270 eV. All Ag crystals showed sharp LEED patterns. In ultra-high-purity Al it is normally sufficient to remove the thin oxide layer on the surface. We did not follow the purity of the Al(110) surface with AES. Nevertheless, we followed the cleaning procedure, which has been found to produce a clean and defect-free surface in the very same crystal.[40]

The possible surface contamination was monitored with AES also during the measurement of e^+ and Ps yields. Moreover, the e^+ and Ps yields turned out to be sensitive to the surface contamination. At the Cu(111)

surface we followed the AES peak intensities and the Ps yield at 30 K after flash heating the surface to above room temperature. Both the Cu Auger intensities and the Ps yield remain practically unchanged for over 30 min, whereafter they decreased, presumably due to hydrogen adsorption. No increase in oxygen or carbon contamination was observed. At low temperatures the measurements were completed within 15 min after cleaning the surface, and care was taken to make sure that there are no changes in the absolute Ps and e^+ yields during this time.

For controlling the sample temperature a closed-cycle He cryocooler installed into a UHV feedthrough and electron beam heating were used. The temperature varies from 20 K up to 1100 K. For the measurement of the sample temperature we use type-*K* (Ni-Cr/Ni-Al) thermocouples affixed to the sample surface. The thermocouples were carefully calibrated at low temperatures against a Au(0.07%)Fe/Ni-Cr thermocouple and a Si diode. For the temperature reference an electrical zero-point reference is used. The error in temperature below 50 K is estimated to be within ± 5 K and at higher temperatures less than 2 K.

IV. RESULTS

A. Cu(111)

For the Cu(111) surface we measured the positronium yields both with the reemitted positrons returned to the surface (f_{Ps}^{+}) and removed from the sample surface and the detector region (f_{Ps}^{-}), allowing us to evaluate the true Ps yield (f_{Ps}) and the thermal reemission yield (f_{e^+}). Although the energy distribution of reemitted thermal positrons was also measured, due to the finite energy resolution and the absence of large-angle emission, the positron work function could only be determined to be $-300\ \mathrm{meV} < \phi_+ < 0$ at room temperature. At higher temperatures it was clearly positive. The transition from the negative to positive work function takes place approximately at 400 K.

Figure 3 shows the experimental positron reemission yields at 30, 70, and 223 K. Apparently, the decrease in temperature from 223 down to 30 K strongly reduces the thermal reemission probability. The nonthermal contribution stays, however, almost independent of the temperature. The solid lines in the figure are least-squares fits to Eqs. (2) and (5a), yielding the thermal reemission yield $f_{e^+}(E)$ and, when extrapolated to zero incident energy, also $f_{e^+}(0)$ at the surface. To extract the contribution of thermal positrons, the low incident positron energy data up to 6 keV were omitted. The positron diffusion length in Cu is taken as $L_+ = [1400(200)]T^{-0.31}$ Å, based upon high statistics line-shape parameter data from 35 to 600 K from the same Cu(111) crystal.[36] We also determined the positron diffusion length L_+ from the Ps fraction data $f_{\mathrm{Ps}}^{+}(E)$. This gives $L_+ = [1350(300)]T^{-0.30}$ Å, in good agreement with the diffusion length in Ref. 36, and the effect of the uncertainty in L_+ on either $f_{e^+}(0)$ or $f_{\mathrm{Ps}}(0)$ is less than 0.02 at any temperature.

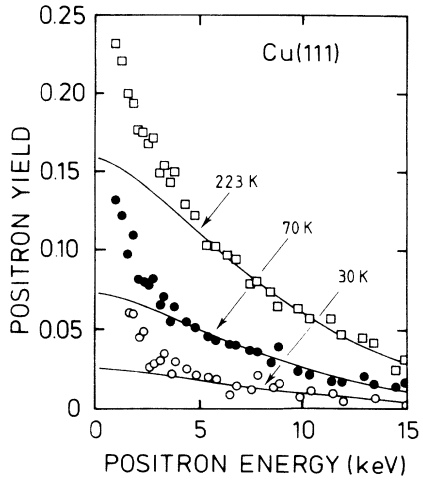

FIG. 3. Reemission yields $f_{e^+}(E)$ for the Cu(111) measured at 30, 70, and 223 K.

The thermal reemission yields, extrapolated to zero incident positron energy, are shown in Fig. 4 from 20 to 600 K. The quoted errors reflect both the statistical errors and the uncertainty in the diffusion length. Below 300 K the thermal reemission yield $f_{e^+}(0)$ is strongly depleted, vanishing as the temperature decreases towards 0 K. At 20 K the reemission yield is less than 0.02, compared with $f_{e^+}(0) \approx 0.20$ around 300 K. The integral reemitted energy distribution measured at the incident positron energy of 3 keV, shown in Fig. 5 at three different temperatures, remains sharp below 300 K. This is characteristic of an elastic escape process leading to a steep slope in the integral distribution, broadened only by the thermal spread of positrons and the instrumental

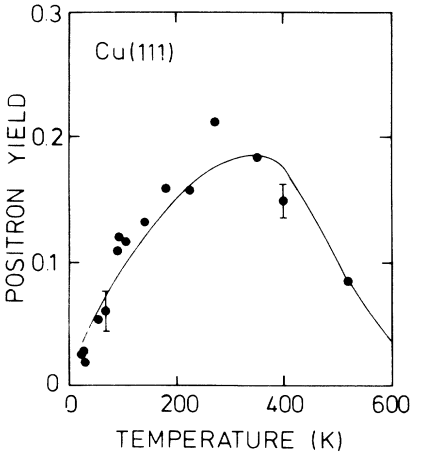

FIG. 4. Reemission yield vs temperature for Cu(111). The solid line corresponds to a least-squares fit to Eq. (6a) assuming that all the temperature dependence is due to reflection from the surface potential. The temperature dependence of the positron work function has been adopted from earlier experimental data (see text).

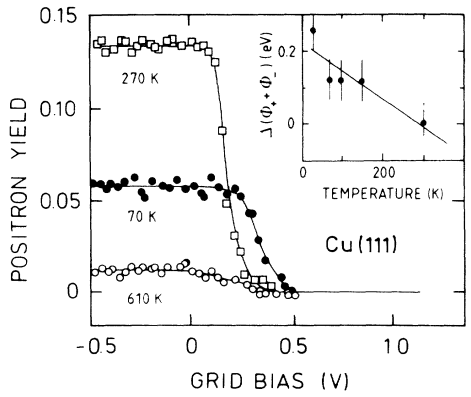

FIG. 5. Integral energy spectrum of reemitted positrons at 70, 270, and 610 K for 3-keV incident positrons. In the inset the relative changes in the positronium formation potential are shown, taking the 300 K value as a reference.

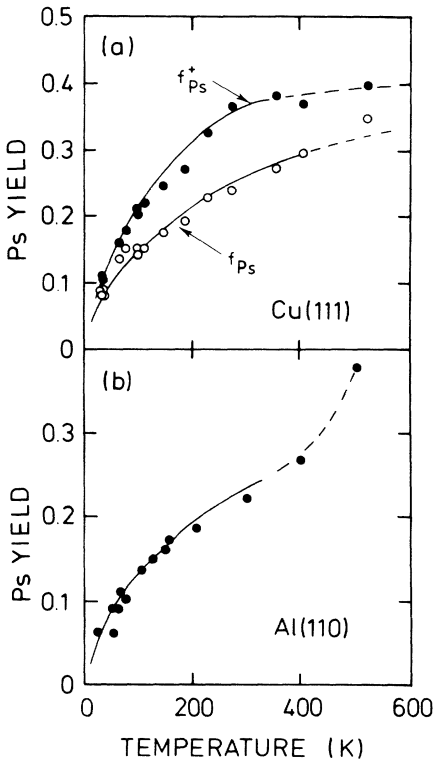

FIG. 6. Ps fractions as a function of temperature for (a) Cu(111) and (b) Al(110). The solid lines correspond to least-squares fits to Eq. (6b), and the dashed lines are a guide for the eye.

resolution. Above 400 K the thermal positron yield gradually falls with increasing temperature. The reduced thermal yield is attributed to the positron work function, which becomes positive, allowing only those positrons at the high-energy tail of the positron energy distribution to escape. This is also seen in the broadened energy distribution of reemitted positrons at 610 K in Fig. 5.

Because of the unknown electron contact potential difference between the sample and the retarding grid, we are not able to extract the absolute positron work function from the integral energy distributions. Nevertheless, we can directly find the temperature variation of the sum of the positron and electron work functions $\phi_+ + \phi_-$ which, apart from the binding energy of a Ps atom in vacuum, is also referred to as the Ps formation potential ϕ_{Ps}. The result is given in the inset of Fig. 5, taking the 300 K value as a reference. Assuming a linear temperature dependence, we find $d(\phi_{Ps})/dT = (8\pm2)\times10^{-4}$ eV/K, in good accord with the Ps formation potential data of Rosenberg *et al.*[41] measured between 300 and 800 K. Later on it will be argued that, because of the very small temperature dependence of the electron work function on a carefully cleaned Cu(111) surface, this temperature variation can to a good approximation be attributed to the positron work function (see Sec. V).

The positronium yield, extrapolated to zero incident positron energy, in the temperature range from 20 to 600 K is shown in Fig. 6(a). We present both the true Ps yield $f_{Ps}(0)$ and the yield $f^+_{Ps}(0)$ measured with the reemitted positrons returned to the sample surface. As for the e^+ reemission data, the incident positron energies less than 6 keV were omitted. The most prominent feature in Fig. 6(a) is a strong reduction in the Ps formation at temperatures below 300 K. Qualitatively, the behavior is very similar to what was observed for thermal positron reemission. Approaching room temperature from below, Ps yields increase until the elastic transmission is at maximum as indicated by the reemission yield. While the reemission yield falls with increasing temperature above 350 K as the work function becomes more positive, the positronium yield $f_{Ps}(0)$ remains approximately constant as the work function changes its sign, until desorption from the surface state occurs. At even higher temperatures (not shown), the Ps yield exhibits the typical behavior of thermally activated desorption from the e^+ surface state, approaching saturation $f_{Ps}(0)\approx1$ at 1100 K.

B. Al(110)

Positron and positronium emission from the Al(110) surface was studied in less detail. Only the Ps yield with all reemitted positrons returned to the sample was determined. The Al(110) is expected to have a small negative positron work function, $\phi_+ = -0.1 - -0.2$ eV, at room temperature, although we have no direct information except that the thermal positron emission is observed, implying that ϕ_+ is negative. In analyzing the Ps emission yield, the positron diffusion length determined both from the Ps fraction and Doppler line-shape measurements[36] was taken as $L_+ = [1600(100)]T^{-0.31}$ Å.

The positronium yield $f^+_{Ps}(0)$ for the Al(110) surface is shown in Fig. 6(b) from 20 to 600 K. As for the Cu(111) surface, the yield is strongly depleted below 200 K, vanishing in the limit $T\rightarrow0$. There is an increasing contribution from thermally desorbed positronium already

around 400 K, implying a smaller activation energy for thermal desorption than that for the Cu and Ag surfaces.

C. Ag(100) and Ag(111)

From the Ag(100) and Ag(111) surfaces no thermal positron emission was observed, indicating a positive positron work function at both surfaces. A positive value of ϕ_+ was verified for the (100) surface from 30 to 700 K, and for the (111) surface from 20 to 300 K. This is in accord with the theoretical values, predicting positive positron work function $\phi_+ = 0.72$ and 0.62 eV at Ag(100) and Ag(111) surfaces, respectively.[42]

As for the Cu and Al data above, the positron diffusion length $L_+ = [1100(100)]T^{-0.32}$ Å measured from one of the Ag(111) crystals was taken from Ref. 36. In analyzing the Ps fraction, the incident positron energies less than 5 keV were omitted.

Figure 7 shows the positronium yields $f_{Ps}(0)$ from the two surfaces from 20 to 600 K. In the case of the Ag(111) surface data are from two separate crystals. Considering the temperatures below 200 K, positronium formation at the Ag(111) and Ag(100) surfaces exhibits a different temperature behavior. At the (111) surface Ps emission falls down, resembling to some extent what is observed at the Cu(111) surface, even if the e^+ work function is positive. Although there is a small decrease in the probability of positronium formation below 100 K at the Ag(100), the Ps yield remains high at the lowest attainable temperature 20 K. The difference between the two surfaces is further demonstrated in Fig. 8, showing the experimental Ps yields at 67 and 76 K at the Ag(111) and Ag(100) surfaces, respectively, with fits to Eq. (2). The diffusion lengths are very nearly equal because of the small difference in temperature, but the positronium fraction is much smaller at the (111) surface, independent of the incident positron energy. As the temperature increases, the difference between the two surface orientations disappears by 200 K. From 300 to 550 K the positronium formation is almost independent of temperature, and the Ps yield is $f_{Ps}(0) = 0.35-0.40$. This is very close to the Ps yield measured at the Cu(111) surface from 500 to 600 K.

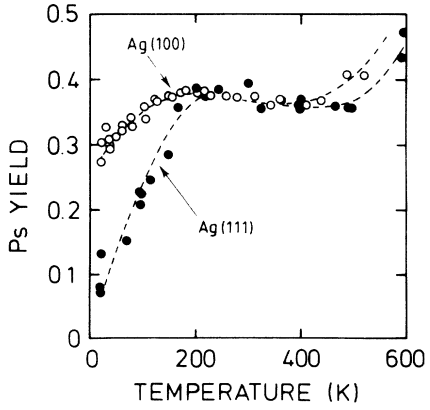

FIG. 7. Ps fractions as a function of temperature for Ag(100) and Ag(111). The dashed lines are a guide for the eye.

The onset of thermally activated desorption from the surface state occurs around 550–600 K leading to a strong increase in Ps emission. At the Ag(100) surface, thermal desorption is observed at a somewhat lower temperature, implying a smaller activation energy than at the Ag(111) surface, consistent with earlier experiments.[43]

V. DETERMINATION OF TRANSITION RATES

A. Negative-work-function surfaces

The results presented in Sec. IV exhibit strongly reduced reemission and Ps yields for negative e^+ work-function surfaces at low temperatures. At Cu(111) the reemission yield $f_{e^+}(0)$ is observed to vanish in the limit $T \to 0$. The temperature dependence may arise from the positron reflection off the surface potential, from competing surface processes or from the temperature-induced variation of the e^+ work function. Reemission has been described[44] in terms of two alternative models, which relate the reemission yield to the positron work function: the e^+ neutralization model, and the density-of-final-states (DOFS) model. If the e^+ work function, which becomes more negative as the temperature decreases is incorporated into these models, both approaches lead to an *increasing* reemission yield at low temperatures. In order to explain the fall in reemission yield, either Ps formation or surface-state trapping rate should increase. Simultaneous Ps yield measurements, however, show a reduction in the yield at low temperatures. On the other hand, surface-state trapping at a negative-work-function surface is mediated by creation of electron-hole pairs, the other processes being less important. This leads to a weak temperature dependence of the capture rate.[22] The experimental observation of vanishing reemission agrees qualitatively with the prediction of increasing reflection of the positron wave from the surface potential.[16]

More surprisingly, Ps formation at the Cu(111) surface shows a temperature behavior very similar to the reemission yield. The same is observed at the other negative-

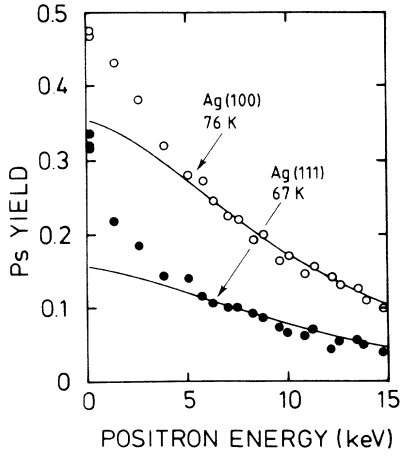

FIG. 8. Ps fractions vs incident energy for Ag(100) at 76 K and for Ag(111) at 67 K. The solid lines correspond to least-squares fits to the diffusion model.

work-function surface, Al(110). This suggests that the wave-mechanical reflection is responsible also for the reduced Ps emission rate at low temperatures. Hence, the transition rate for reemission and Ps emission are written in terms of the transmission coefficient $\mathcal{T}$ as

$$\nu_{e^+}=(1-P)\nu_0\mathcal{T} \quad \text{and} \quad \nu_{\mathrm{Ps}}=P\nu_0\mathcal{T} . \tag{10}$$

P is the intrinsic probability for a positron to pick up an electron at the surface to form a Ps atom,[16] and ν_0 is a constant. The elastic transmission rate is given by the transmission coefficient as $\nu_T=\nu_0\mathcal{T}$. This explicitly assumes that the observed temperature dependencies are attributed solely to the transmission probability, apart from the relatively weak temperature effect on the pickup probability P (see Sec. VI).

In the following our purpose is to examine whether the transmission coefficient can account for the observed temperature behavior, making use of the reflection of a plane wave off the effective single-particle potential for a positron near the surface. Equation (6) is fitted to the experimental reemission and Ps yields to estimate the transition rates. ν_S is assumed to be constant as the capture rate into the surface state depends only weakly on the temperature for negative-work-function surfaces.[22] When the transition rates ν_{e^+} and ν_{Ps} in Eq. (10) are incorporated into Eq. (6), three temperature-independent parameters are left: ν_0, ν_S, and P. If the reemission and Ps yields are summed, the pickup probability P cancels, allowing for a least-squares fit with only two free parameters.

The effective single-particle potential near the surface is schematically depicted in Fig. 1. At the surface, the positron is subject to a potential step, the height of which is equal to $-\phi_+$. The magnitude of ϕ_+ is determined by the surface dipole and the chemical potential, which consists of the positron interaction energies with ion cores and surrounding electrons. Outside the surface a smooth mirror potential, having a long-range $1/4(z-z_0)$-tail cutoff at a minimum value corresponding to the Ps binding energy (6.8 eV), gives a good description of the nonlocal image-charge interaction by an appropriate choice of the image-plane position z_0.[45] The image potential is joined to the positron energy level inside the crystal by a smoothly varying function. Alternatively, we have described the positron surface potential with a simple square step. The positron state inside the crystal is represented by a plane wave.

In calculating the transmission coefficients, the thermal energy distribution of positrons is included. Further, in the case of Cu(111), the temperature dependence of the e^+ work function has been taken into account. Rosenberg *et al.*[41] have measured the temperature dependence of the Ps formation potential ϕ_{Ps}. They found for Cu $d\phi_{\mathrm{Ps}}/dT=7.3\times10^{-4}$ eV/K above room temperature. This is in good agreement with our peak shifts (see Sec. IV), which measure the same temperature dependence, showing a slope of $(8\pm2)\times10^{-4}$ eV/K between 20 and 300 K. For the electron work function at Cu(111) the experimental temperature coefficients $d\phi/dT=-(10\pm6)\times10^{-5}$ eV/K (Ref. 46) and $d\phi/dT=-8\times10^{-5}$ eV/K (Ref. 47) have been reported. The values are in good agreement with a theoretical estimate of Kiejna, $d\phi/dT=-15\times10^{-5}$ eV/K.[48] If these values are combined with the positronium data,[41] the temperature coefficient for the e^+ work function at the Cu(111) surface is $d\phi_+/dT=8.6\times10^{-4}$ eV/K, which is an order of magnitude larger than that of electrons. This value agrees well with that obtained by Murray *et al.*[32] for a sulphur-covered Cu(111), $d\phi_+/dT=(8.8\pm0.4)\times10^{-4}$ eV/K, even though they did not observe any temperature dependence for a clean Cu(111) surface. We have taken the temperature coefficient to be $d\phi_+/dT=8\times10^{-4}$ eV/K. For Al(110), a constant e^+ work function is assumed due to the lacking experimental values.

Figure 9 shows the transmission coefficient $\mathcal{T}$ as a function of temperature for the image potential. The positron work function and the mirror plane position correspond to those of the Cu(111) surface (Tables I and II). For any choice of the potential, the transmission is observed to vanish as $T\rightarrow0$. The inclusion of the thermal energy distribution is found to increase the transmission to some extent, but it does not influence the overall temperature behavior. Further, the transmission probability is only weakly influenced by the temperature variation of ϕ_+ except that a clear cutoff, similar to that observed in the reemission at Cu(111), is seen as the e^+ work function becomes positive. The transmission probability of a plane wave with kinetic energy $k_BT/2$ (k_B is the Boltzmann constant) through a step potential can be solved analytically and is expressed as

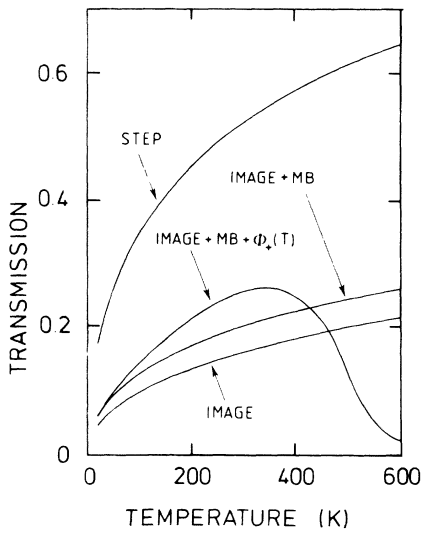

FIG. 9. Calculated transmission vs temperature for Cu(111) surface potential assuming a simple step potential, assuming a constant image potential, assuming a constant image potential with Maxwell-Boltzmann energy distribution for a positron and further incorporating the temperature-dependent work function to the previous one.

TABLE I. Notations for the measured fractions and transition rates.

$f_{Ps}^{+}(E)$	Positronium fraction from Eq. (8) as the reemitted positrons are returned to the sample
$f_{Ps}^{-}(E)$	Positronium fraction from Eq. (8) as the reemitted positrons are allowed to escape the detector region
$f_{Ps}(E)$	Fraction of positrons emitted from the surface as a Ps atom
$f_{e^+}(E)$	Fraction of reemitted positrons
$f_{sum}(E)$	$f_{Ps}(E)+f_{e^+}(E)$
ν	Total transition rate out of the bulk state
ν_S	Transition rate for the capture into the surface state
ν_T	Transition rate through the surface potential
ν_{e^+}	Transition rate for the reemission
ν_{Ps}	Transition rate for the Ps emission

$$\mathcal{T}=\frac{2\sqrt{kT(kT-2\phi_+)}}{kT-\phi_+ +\sqrt{kT(kT-2\phi_+)}} . \quad (11)$$

A step potential produces a qualitatively similar T dependence as the image potential, but its transmission probability is much higher. In the case of the image potential the transmission coefficient is calculated numerically.

In Table III estimates for the transition rates ν_0 and ν_S are given for Cu(111) and Al(110). In the case of the Cu(111) surface, the most reliable estimates are extracted from the combined yield f_{sum}, which does not contain any contribution from the pickup probability. To a good approximation, the transmission coefficient $\mathcal{T}(T)$ reproduces the temperature behavior below 400 K, assuming constant rates ν_0 and ν_S, as shown in Fig. 10. Results from fitting the e^+ and Ps yields separately are given in Table III for comparison. The overall temperature behavior of the reemission yield, shown in Fig. 4, can also be explained by the model. The inclusion of the thermal energy distribution is needed to reproduce the high-temperature reemission data. In the case of Ps yield we omitted the data above 350 K, since the Ps emission cannot be described by simple transmission when the e^+ work function becomes positive.

The capture rate into the surface state is found to be of the order of $\nu_S \sim 10^3$ m/s, and the transition rate ν_0 an order of magnitude higher, $\nu_0 \sim 10^4$ m/s.[49] Considering the e^+ and Ps yields separately, a reasonable description of the data is obtained taking the transition rates from f_{sum} fits and assuming a constant pickup probability P.

TABLE II. Parameters used to model the surface potential for negative-work-function surfaces.

	Cu(111)	Al(110)
Work function ϕ_+	-0.375 eV $+[0.8T/(1\ K)]$ (1 meV)	-0.19 eV
Mirror plane position z_0	0.55 Å	0.65 Å

TABLE III. The estimated transition rates for Cu(111) and Al(110). We have assumed pickup probabilities $P=0.6$ for Cu and $P=0.5$ for Al.

	Cu(111)	Al(110)
f_{sum}	$\nu_0=(6300\pm500)$ m/s $\nu_S=(700\pm200)$ m/s	
f_{e^+}	$\nu_0=(4500\pm1600)$ m/s $\nu_S=(100\pm500)$ m/s	
f_{Ps}	$\nu_0=(7800\pm500)$ m/s $\nu_S=(1300\pm200)$ m/s	
f_+	$\nu_0=(14300\pm1600)$ m/s $\nu_S=(680\pm100)$ m/s	$\nu_0=(3500\pm200)$ m/s $\nu_S=(600\pm100)$ m/s

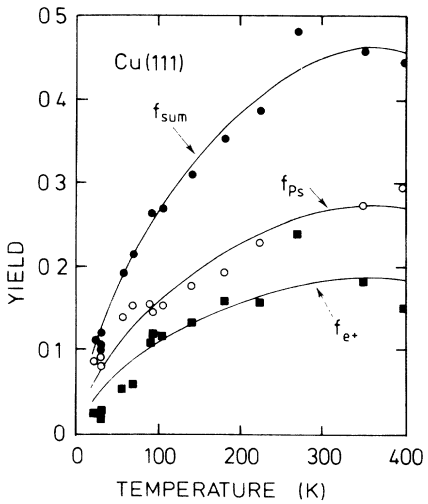

FIG. 10. f_{sum}, f_{Ps}, and f_{e^+} measured as a function of temperature for Cu(111). Solid lines correspond to the least-squares fits to results. For the f_{sum} curve we obtained values $\nu_0=(6300\pm500)$ m/s and $\nu_S=(700\pm200)$ m/s. These values were fixed in the other two fits, and pickup probability P was fitted. For P we obtained a value $P=0.59$ from both the f_{Ps} and f_{e^+} data.

The reemission data yield $P=0.59\pm0.10$, and correspondingly from the Ps emission $P=0.59\pm0.06$ (shown in Fig. 10). These values lead to the room-temperature transition rates $\nu_{e^+}\approx 650$ m/s and $\nu_{Ps}\approx 930$ m/s, indicating that the reemission, the Ps emission, and the surface-state trapping are equally probable. From Eq. (2), a rough estimate for the overall escape probability at 300 K is $J(0)\sim 0.7$.

For Al(110) only the f_{Ps}^{+} data were measured. Assuming the pickup probability $P=0.5$, the transition rates $\nu_0=3500\pm200$ m/s and $\nu_S=600\pm100$ m/s are obtained. The values are comparable to the corresponding values of Cu(111). The data below 400 K were again included into the fit. For both surfaces the transition rate ν_0 of a simple square step is somewhat lower than for the image potential. This arises directly from the higher transmission through the step potential.

B. Positive-work-function surfaces

At the Ag(100) and Ag(111) surfaces the reemission is prohibited because of the positive e^+ work function. The previous arguments assuming that the Ps formation follows the elastic escape of the positron are no more valid, and the effect of the reflection is less obvious when ϕ_+ is positive. Considering the Ag(100) surface, the results in Fig. 7 would imply a weak temperature dependence of Ps formation at a positive-work-function surface. This is supported by the nearly constant Ps yield above 200 K at both surfaces. Assuming this is the case also at the Ag(111) surface, the seemingly strong temperature dependence below 200 K can be explained by invoking a new mechanism for the capture into the surface state.

Thus we tentatively choose the Ag(100) data to be the starting point of our analysis. ν_{Ps} is assumed to be constant, and ν_S is taken to be a weak, linear function of temperature according to the theoretical calculations for the electron-hole-pair mediated surface-state trapping.[22] Under these assumptions, the least-squares fit of the observed Ps emission yield of Ag(100) to Eq. (6) with $\nu_{e^+}=0$ leads to the transition rates $\nu_{Ps}=970\pm30$ m/s and $\nu_S(T)=[(1390\pm90)+(1.1\pm0.5)\ \mathrm{T/K}]$ m/s. The surface trapping rate is consistent with the theoretical estimates of Kong *et al.*,[22] which give the trapping rate of $\nu_S(T)\approx(5000+0.5\ \mathrm{T/K})$ m/s for a somewhat different surface potential.

The Ps emission rate $\nu_{Ps}=930$ m/s is adopted also for the Ag(111). This leads to a strongly enhanced surface-state capture rate ν_S at low temperatures, shown in Fig. 11. The rate is increased by an order of magnitude as the temperature decreases from 200 to 20 K, inconsistently with the model of electron-hole-pair assisted trapping. This suggests a new transition mechanism to be present at the Ag(111) surface.

Kong *et al.*[22] have explored the possibility of the acoustic-phonon-mediated trapping. They find that in some cases a high-lying surface state may act as a precursor state for trapping into the deep surface traps. This requires that the energy level of the positron in the solid is within the phonon energy from the high-lying bound state at the surface well. Being accessible through the phonon emission, the capture rate is strongly temperature dependent. Furthermore, the high-lying precursor state becomes unstable at relatively low temperatures due to thermal desorption. Qualitatively, the acoustic-phonon-assisted surface trapping leads to a strongly enhanced surface trapping rate, similar to that depicted in Fig. 11. The rather restrictive condition of the e^+ energy level being within the phonon energy above the bound precursor state would also give an explanation to the fact that a small difference (~ 0.1 eV) in the e^+ work function leads to totally different temperature behavior at the Ag(100) and Ag(111) surfaces.

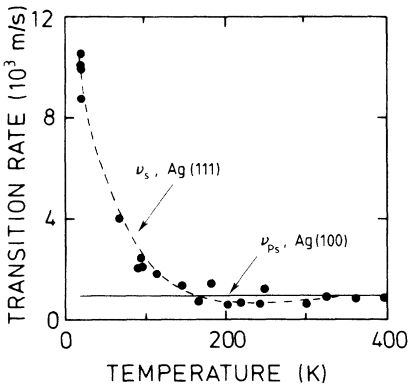

FIG. 11. Positronium emission rate for the Ag(100) obtained from a least-squares fit as a function of temperature assuming the rate to be temperature independent (solid line). The transition rate is $\nu_{Ps}=970$ m/s. The black dots correspond to the calculated surface trapping rate for Ag(111) assuming $\nu_{Ps}=970$ m/s. The dashed line is a guide for the eye.

VI. DISCUSSION

A. Negative-work-function surfaces

The importance of the positron reflection was first suggested by Nieminen and Oliva.[16] They argued that the escape probability from a negative-work-function surface vanishes at low temperatures. This would leave trapping into the surface state the only escape channel. The early experiments failed to observe this effect. Measurements of both the Ps (Ref. 18) and the e^+ (Ref. 17) emission probabilities for the Cu(111)+S surface showed nearly constant yields below 600 K. This discrepancy has been explained by the dominance of inelastic escape processes[50] or by allowing the reflected positron many encounters with the surface.[51]

In the present work, however, we have observed the reemission probability from Cu(111) to be strongly reduced at low temperatures. Positron reemission has been described in terms of the resonant electron transfer during the surface transmission[44,52] and by relating the emission probability to the density of final states of the ejected positron.[8,44] These models correlate the e^+ emission to the magnitude of the e^+ work function. Gullikson *et al.*[44] have measured the reemission yield for Cu(111)

and Ni(100) surfaces at room temperature, varying systematically the work function ϕ_+. The reemission rate increases as ϕ_+ becomes more negative, consistently with the DOFS or the resonant-electron-transfer model. This would lead to *increasing* reemission at Cu(111) at low temperatures. The reduced reemission yield, opposite to what is predicted from the e^+ work-function change, indicates that the most important contribution to the temperature dependence arises from the reflection. Moreover, the transmission probability at a constant temperature is only weakly affected by a small change in ϕ_+, explaining why the effect of reflection cannot be observed in the results of Ref. 44.

The absolute reemission yields at the Cu(111) differ between those measured by Gullikson *et al.*,[44] showing a yield of 0.4 at 300 K, and those given in Fig. 4. The origin for this difference is in the e^+ work function, which they found to be more negative, $\phi_+ = -0.4$ eV, presumably due to the presence of S on the surface.[32] We believe the work function to be $\phi_+ \approx -0.1$ eV at 300 K, supported by the fact that ϕ_+ changes it sign between 350 and 400 K. The absolute reemission yield $f_{e^+}(0) = 0.20$ at 300 K agrees with that measured at the same work function in Ref. 44. All these observations support the picture of reemission being a simple elastic escape process through the surface potential.

The positronium yield at Cu(111), similar to the Al(110) surface, closely resembles the reemission yield as a function of temperature. From this similarity we anticipate that the temperature dependence of the Ps formation and reemission at low T have the same origin. Time-of-flight[11,29,53] and two-dimensional angular-correlation[5] measurements give evidence that to a good approximation the formation of a Ps atom at the surface is a sudden process, with capture of a single electron from the metal allowing for a simple interpretation in terms of a single-particle picture. The Ps formation potential ϕ_{Ps} extracted from the TOF measurements is -2.5 and -2.8 eV at the Cu and Al surfaces, respectively,[29] in close agreement with those predicted from the electron and positron work functions. By energy conservation, only electrons between the Fermi level (E_F) and $E_F + \phi_{Ps}$ can participate in the Ps emission. Ps formation has been described in terms of models derived from the ion-neutralization theories[16,54,55] and models closely resembling photoemission.[56] None of these models predicts any strong intrinsic temperature dependence in Ps emission. The temperature variation of the positron work function and the Ps formation potential undoubtedly induce temperature-dependent factors, e.g., by changing the intrinsic electron pickup probability or the ensemble of electrons participating the Ps formation. However, as already suggested by the remission data, effects related to the positron and electron work functions are of minor importance and the temperature dependence of both e^+ and Ps emission at low temperatures is dominated by the reflection of the positron wave, independent of the detailed process of the Ps formation.

Similarity between the temperature behavior of reemission and Ps formation further suggests that the formation and emission of the Ps atom consists of two separate processes: transmission through the surface potential, and the electron pickup. This division to steplike processes is analogous to the three-step model of photoemission.[57] Although the analogy between photoemission and Ps emission has been an item of speculation,[24] recent two-dimensional angular correlation of annihilation radiation (2D-ACAR) observations show certain dissimilarities attributed to the different excitation mechanisms.[5] In photoemission, electrons are excited optically, whereas in Ps emission the electron escape is assisted by the energy released in forming the Ps atom (-6.8 eV). The strong electron-positron interaction changes the process from the photoemission. Recently Ishii and Pendry have given a description of Ps formation closely resembling the photoemission theories.[56] Another surface process, which has analogies to the Ps emission, is the ion neutralization. The theories developed in that context[58] have been adopted and developed to describe Ps formation.[16,54,55]

The existence of the positron surface state was first predicted by Hodges and Stott.[13] There have been several theoretical attempts to estimate the surface-state trapping rate starting from the golden-rule approach. Electron-hole-pair excitation has been found to be the dominating mechanism for trapping at least at the negative-work-function surfaces. Nieminen and Laakkonen obtained for the Al surface state the trapping rate $\nu_S = 7600$ m/s. Other estimates have given consistent values between 10^3 and 10^4 m/s.[16,21,22] Making use of the simple approach of a plane-wave reflection from the effective single-particle potential for the positron near the surface, we have attained the first experimental estimates for the transition rates. For the trapping into the surface state we find the transition rate of the order $\nu_S \sim 10^3$ m/s, in good agreement with the theoretical predictions. The transition rate ν_0 is of the order of 10^4 m/s, and these values lead to the room-temperature transition rates $\sim 10^3$ m/s for e^+ and Ps emission, indicating that the different escape processes exhibit almost equal probabilities, which is a relatively general observation for metals where ϕ_+ is negative.

Recently Jensen *et al.*[59] have performed positron-lifetime measurements on Cu samples containing Kr-filled micrometer-size cavities. They found that positrons are trapped at the cavity surfaces, and that the trapping cannot be explained with a diffusion-limited model alone. From those experiments an estimate $\nu_S \approx 1100 \pm 600$ m/s for the surface trapping rate was deduced, in good accord with our results. This value, as well as our results, seems to be lower than theoretical numbers.[20,21,22] This could be merely a coincidence, but also a shortcoming of the static golden-rule model.

Even if the model is oversimplified, the reemission or Ps emission allows for a description in terms of a simple, textbook example of a plane-wave reflection from a static one-dimensional single-particle potential, independent of the details of the omission process. The positron approaching the surface is more properly described as a wave packet, which is strongly correlated with the surrounding electrons. Some of the many-body effects are, however, incorporated into the model. The positron

work function, determining the step height at the surface, has a contribution from the correlation energy, and the mirror potential gives a reasonable description of the nonlocal image interaction. The success of the simple model suggests that many-body phenomena and dynamical effects are likely to be small.

The controversy between earlier measurements and our results originates for the most part from differences in data analysis. During the time of the earlier experiments, the understanding of the positron-surface interaction was incomplete. The knowledge of positron implantation and diffusion was inaccurate and, in particular, nonthermal effects[34] were not fully accounted. Furthermore, the Cu samples studied in Refs. 17 and 18 were partially sulphur covered, which was reported to lead to a large and reverse temperature dependence of ϕ_+.[17] In those measurements no surface analysis with AES was performed below room temperature. However, we cannot definitely point out from where the difference in results arises.

B. Positive-work-function surfaces

At the positive-work-function surfaces there are two escape channels available for positrons: emission as a Ps atom, or trapping into the surface state. The role of reflection is not so obvious, and the Ps emission is associated with the overlap of the e^+ wave function with the low-electron-density tail outside the surface, which is observed to result in the Ps yields comparable to negative-work-function surfaces. This is also demonstrated at the Cu(111) surface, where the change in the sign of ϕ_+ around 350 K leaves the Ps yield practically unaffected.

The Ps yield at the Ag(100) surface remains relatively high even at 20 K, whereas the Ag(111) surface shows a rapid decrease in Ps emission rate below 200 K. Since both Ag(100) and Ag(111) have almost equal positive work functions, and the Ps formation potential is large and does not depend on the crystal orientation, there are no apparent reasons why the Ps formation should differ between Ag surfaces.

Another principal reason for the temperature dependence is the enhanced capture rate into the surface state. Kong *et al.*[22] have looked for this possibility considering phonon-assisted trapping. It is found that, in some cases, the high-lying Rydberg-like states can act as precursor states, analogous to trapping at negatively charged vacancies in semiconductors.[60] This requires that the delocalized positron state inside the crystal is within the phonon energy above the Rydberg surface state. Being accessible through phonon emission, the capture rate becomes strongly enhanced at low temperatures. Moreover, at high temperatures, thermal desorption makes the precursor states ineffective, and no difference between the (100) and (111) surfaces is expected. If the trapping via the precursor state is possible at the Ag(111) but not at the Ag(100) surface, a decreased Ps yield is observed at low temperatures at the Ag(111) surface. It would also imply that at positive-work-function surfaces the effects of reflection of the positron wave are weak. When the electron-hole-assisted transition is the only channel for capture to the surface state, the overall Ps formation has a weak temperature dependence, as observed at the Ag(100) surface. However, as the experimental data from the Ps formation at positive-work-function metal surfaces at low temperatures is limited to the present work, it is not possible definitely to decide the origin of the observed temperature behavior. The only other study of temperature dependence of Ps formation from the $\phi_+ > 0$ surface below room temperature has been done by Sferlazzo *et al.*[61] from graphite, where they observe totally different linearly increasing Ps formation probability, which is interpreted in terms of acoustic-phonon-assisted Ps formation.

Kong *et al.* have also calculated the temperature dependence of electron-hole-pair assisted surface-state trapping for deep surface states.[22] Temperature dependence is found to be approximately linear, and for a state with binding energy $E_b = 1.77$ eV they get slope of ~ 0.5 m/s K, which is in agreement with that obtained in the present study for Ag(100).

In the present work we have systematically studied the temperature dependence of positron branching at metal surfaces. However, we are still lacking some basic data of positron surface processes from simple metal surfaces. Simultaneous determination of e^+ and Ps yields from a representative set of samples with different e^+ work functions should prove worthwhile. Also, the temperature dependence of the e^+ work function, especially at low temperatures, has obtained inadequate attention. Further, it must be denoted that we determine ν_S indirectly from e^+ and Ps yield data. The direct evaluation is not possible with the present technique, but as, e.g., the positron lifetime techniques[62] are developed, the surface trapping fraction can be measured by changes in the intensity of surface lifetime.

Phenomena occurring while a low-energy light atom interacts with a surface have been a widely studied subject. For example, the value of the sticking coefficient for low-energy helium scattering at low temperatures is a long-standing problem.[23,63,64] Sticking of spin-polarized hydrogen has also been an item of interest.[65–67] In particular, the quantum nature of the surface processes has become of interest. Positrons, as well as positronium, may prove to be useful probes in this context.

VII. CONCLUSIONS

We have studied the temperature dependence of different positron interactions at metal surfaces. Reemission and positronium yields have been determined at Cu(111), Al(110), Ag(100), and Ag(111) surfaces from 20 up to 1000 K. Our main results can be summarized as follows.

1. For negative-work-function surfaces, we find that both Ps and e^+ emission show similar temperature dependence. At low temperatures the transition rates become smaller, vanishing in the limit $T \rightarrow 0$. Reemission from Cu(111) is observed to be an elastic process, the temperature dependence of which can be explained by

quantum-mechanical transmission through the surface potential. As temperature increases, the reemission starts to reduce again at 400 K, where the work function for Cu(111) becomes positive. Ps emission from Cu(111) and Al(110) is found to obey similar T dependence. This suggests that Ps formation can be described with two distinct steps: the transmission through the surface potential, and the electron capture at the low-electron-density tail just outside the surface.

2. All results from negative-work-function surfaces can be modeled with a simple plane wave interacting with a one-dimensional single-particle surface potential. Temperature dependence of both e^+ and Ps emission can be totally attributed to positron transmission through the potential. Using the model, we find that reemission, Ps emission, and surface-state trapping to have approximately equal strengths, and the transition rates are of the order of $\nu \sim 10^3$ m/s.

3. For Ag(100) and Ag(111), both having positive work function, we observe different temperature behavior below 200 K. The Ag(111) data can be explained by the acoustic-phonon-mediated trapping into a high-lying Rydberg state, which acts as a precursor state for trapping into deeper states. At the Ag(100) surface, this mechanism is not energetically possible, i.e., the energy loss is too large for phonon emission, and the electron-hole trapping is the only possibility, with a much weaker temperature dependence.

ACKNOWLEDGMENTS

We thank R. M. Nieminen, M. Puska, Y. Kong, A. Walker, and K. O. Jensen for useful discussions. Work performed at Helsinki University of Technology was partially supported by the Academy of Finland and the Royal Society.

---

*Present address: Outokumpu Electronics, P.O. Box 85, SF-02201 Espoo 20, Finland.

†Present address: Institute for Nuclear Solid State Physics, University of Bundeswehr München, Werner-Heisenberg-Weg 39, D-8014 Neubiberg, FRG.

‡Present address: Department of Applied Sciences, Brookhaven National Laboratory, Upton, NY 11973-5000.

§Present address: Outokumpu Group, P.O. Box 280, SF-00101 Helsinki 10, Finland.

[1]P. J. Schultz and K. G. Lynn, Rev. Mod. Phys. **60**, 701 (1988).

[2]I. J. Rosenberg, A. H. Weiss, and K. F. Canter, Phys. Rev. Lett. **44**, 1139 (1980).

[3]D. A. Fischer, K. G. Lynn, and W. E. Frieze, Phys. Rev. Lett. **50**, 1149 (1983).

[4]A. Weiss, R. Mayer, M. Jibaly, C. Lei, D. Mehl, and K. G. Lynn, Phys. Rev. Lett. **61**, 2245 (1988).

[5]D. M. Chen, S. Berko, K. F. Canter, K. G. Lynn, A. P. Mills, Jr., L. O. Roellig, P. Sferlazzo, M. Weinert, and R. N. West, Phys. Rev. B **39**, 3966 (1989).

[6]A. Vehanen, J. Mäkinen, P. Hautojärvi, H. Huomo, J. Lahtinen, R. M. Nieminen, and S. Valkealahti, Phys. Rev. B **32**, 7561 (1985).

[7]A. P. Mills, Jr., P. M. Platzman, and B. L. Brown, Phys. Rev. Lett. **41**, 1076 (1978).

[8]D. A. Fischer, K. G. Lynn, and D. W. Gidley, Phys. Rev. B **33**, 4479 (1986).

[9]E. M. Gullikson, A. P. Mills, Jr., W. S. Crane, and B. L. Brown, Phys. Rev. B **32**, 5484 (1985).

[10]K. F. Canter, A. P. Mills, Jr., and S. Berko, Phys. Rev. Lett. **33**, 7 (1974).

[11]A. P. Mills, Jr., L. Pfeiffer, and P. M. Platzman, Phys. Rev. Lett. **51**, 1085 (1983).

[12]K. G. Lynn, Phys. Rev. Lett. **43**, 391 (1979).

[13]C. H. Hodges and M. J. Stott, Solid State Commun. **12**, 1153 (1973).

[14]R. M. Nieminen and M. J. Puska, Phys. Rev. Lett. **50**, 281 (1983).

[15]P. M. Platzman and N. A. Tzoar, Phys. Rev. B **33**, 5900 (1986).

[16]R. M. Nieminen and J. Oliva, Phys. Rev. B **22**, 2226 (1980).

[17]P. J. Schultz and K. G. Lynn, Phys. Rev. B **26**, 2390 (1982).

[18]K. G. Lynn, P. J. Schultz, and I. K. MacKenzie, Solid State Commun. **38**, 473 (1981).

[19]D. T. Britton, P. A. Huttunen, J. Mäkinen, E. Soininen, and A. Vehanen, Phys. Rev. Lett. **62**, 2413 (1989).

[20]R. M. Nieminen and J. Laakkonen, Appl. Phys. **20**, 181 (1979).

[21]A. Walker, private communication.

[22]Y. Kong, R. M. Nieminen, P. A. Huttunen, A. Vehanen, and J. Mäkinen (unpublished).

[23]V. U. Nayak, D. O. Edwards, and N. Masuhara, Phys. Rev. Lett. **50**, 990 (1983); M. Sinvani, M. W. Cole, and D. L. Goodstein, *ibid.* **51**, 188 (1983).

[24]R. H. Howell, in *Atomic Physics with Positrons,* edited by J. W. Humberston and E. A. G. Armour (Plenum, New York, 1987).

[25]D. J. O'Connor, Y. G. Shen, J. M. Wilson, and R. J. MacDonald, Surf. Sci. **197**, 277 (1988).

[26]T. McMullen, in *Positron Annihilation, Proceedings of the 7th International Conference on Positron Annihilation, New Delhi, 1985,* edited by P. C. Jain, R. M. Singru, and K. P. Gopinathan (World Scientific, Singapore, 1985), p. 657.

[27]S. Valkealahti and R. M. Nieminen, Appl. Phys. A **32**, 95 (1983); **35**, 51 (1984).

[28]A. Vehanen, K. Saarinen, P. Hautojärvi, and H. Huomo, Phys. Rev. B **35**, 4606 (1987).

[29]R. H. Howell, I. J. Rosenberg, M. J. Fluss, R. E. Goldberg, and R. B. Laughlin, Phys. Rev. B **35**, 5303 (1987).

[30]H. Schut, A. van Veen, B. Nielsen, and K. G. Lynn (unpublished).

[31]P. J. Schultz, K. G. Lynn, W. E. Frieze, and A. Vehanen, Phys. Rev. B **27**, 6626 (1983).

[32]C. A. Murray, A. P. Mills, Jr., and J. E. Rowe, Surf. Sci. **100**, 647 (1980).

[33]V. W. Hughes, S. Marder, and C. S. Wu, Phys. Rev. **98**, 1840 (1955).

[34]H. Huomo, A. Vehanen, M. D. Bentzon, and P. Hautojärvi, Phys. Rev. B **35**, 8252 (1987).

[35]P. A. Huttunen and A. Vehanen (unpublished).
[36]E. Soininen, H. Huomo, P. A. Huttunen, J. Mäkinen, A. Vehanen, and P. Hautojärvi, Phys. Rev. B **41**, 6227 (1990).
[37]B. Bergersen, E. Pajanne, P. Kubica, M. J. Stott, and C. H. Hodges, Solid State Commun. **15**, 1377 (1974).
[38]J. Lahtinen, A. Vehanen, H. Huomo, J. Mäkinen, P. Huttunen, K. Rytsölä, M. Bentzon, and P. Hautojärvi, Nucl. Instrum. Methods Phys. Res. Sect. **17**, 73 (1986).
[39]R. G. Musket, W. McLean, C. A. Colmenares, D. M. Makowiecki, and W. J. Siekhaus, Appl. Surf. Sci. **10**, 143 (1982).
[40]J. Mäkinen, A. Vehanen, P. Hautojärvi, H. Huomo, J. Lahtinen, R. M. Nieminen, and S. Valkealahti, Surf. Sci. **175**, 385 (1986).
[41]I. J. Rosenberg, R. H. Howell, and M. J. Fluss, Phys. Rev. B **35**, 2083 (1987).
[42]O. V. Boev, M. J. Puska, and R. M. Nieminen, Phys. Rev. B **36**, 7786 (1987).
[43]K. G. Lynn and D. O. Welch, Phys. Rev. B **22**, 99 (1980).
[44]E. Gullikson, A. P. Mills, Jr., and C. A. Murray, Phys. Rev. B **38**, 1705 (1988).
[45]M. Puska and R. M. Nieminen, Phys. Scripta **T4**, 79 (1983).
[46]P. O. Gartland, S. Berge, and B. J. Slagsvold, Phys. Norv. **7**, 39 (1973).
[47]G. A. Haas and R. E. Thomas, J. Appl. Phys. **48**, 86 (1977).
[48]A. Kiejna, Surf. Sci. **178**, 349 (1986).
[49]The absolute transition rates given in Ref. 16 are erroneous by 2 orders of magnitude. This, however, does not influence the interpretation of the results.
[50]R. J. Wilson, Phys. Rev. B **27**, 6074 (1983).
[51]D. Neilson, R. M. Nieminen, and J. Szymanski, Phys. Rev. B **33**, 1567 (1986).
[52]M. L. Yu and N. D. Lang, Phys. Rev. Lett. **50**, 127 (1980).
[53]A. P. Mills, Jr., E. D. Shaw, R. J. Chicester, and D. M. Zuckerman, Phys. Rev. B **40**, 8616 (1989).
[54]A. Ishii, Phys. Rev. B **36**, 1853 (1987).
[55]S. Shindo and A. Ishii, Phys. Rev. B **35**, 8360 (1987).
[56]A. Ishii and J. B. Pendry, Surf. Sci. **209**, 23 (1989).
[57]C. N. Berglund and W. E. Spicer, Phys. Rev. **136**, A1030 (1964).
[58]D. M. Newns, Phys. Rev. **178**, 1123 (1969).
[59]K. O. Jensen, M. Eldrup, S. Linderoth, and J. H. Evans, J. Phys. Condens. Matter (to be published).
[60]M. J. Puska, C. Corbel, and R. M. Nieminen, Phys. Rev. B **41**, xxxx (1990).
[61]P. Sferlazzo, S. Berko, K. G. Lynn, A. P. Mills, Jr., L. O. Roellig, A. J. Viescas, and R. N. West, Phys. Rev. Lett. **60**, 538 (1988).
[62]D. Schöldbauer, G. Kögel, P. Sperr, and W. Trifthäuser, Phys. Status Solidi A **102**, 549 (1987).
[63]D. Goodstein, in *Many-Body Phenomena at Surfaces,* edited by D. Langreth and H. Suhl (Academic, New York, 1984).
[64]F. O. Goodman and N. Garcia, Phys. Rev. B **33**, 4560 (1986).
[65]R. Jochemsen, M. Morrow, A. J. Berlinsky, and W. N. Hardy, Phys. Rev. Lett. **47**, 852 (1981).
[66]J. A. Yaple and R. A. Gueyr, Phys. Rev. B **27**, 1629 (1983).
[67]J. J. Berkhout, E. J. Wolters, R. van Roijen, and J. T. M. Walraven, Phys. Rev. Lett. **57**, 2387 (1986).